GeoAmericas2020
4th PAN AMERICAN CONFERENCE ON GEOSYNTHETICS
26-29 APRIL 2020 • RIO DE JANEIRO • BRAZIL

Deformation Analysis of Rails on Geocell Reinforced Earth Beds Under Moving Load

Shashank Bhatra, Department of Civil Engineering, National Institute of Technology Uttarakhand, Sumari
Priti Maheshwari, Department of Civil Engineering, Indian Institute of Technology Roorkee, Roorkee

ABSTRACT
An attempt has been made herein to analyze the rails resting on earth beds with geocell inclusion under a moving load. Reinforced soil system comprises of a granular fill layer (modelled as Pasternak shear layer) followed by a geocell inclusion (represented by an infinite beam with finite bending stiffness) overlying the foundation soil (modelled as a series of spring and dashpot connected in parallel). The governing differential equations have been developed and converted for general use in non-dimensional form. These equations are solved using suitable boundary conditions and employing Finite Difference Scheme along with iterative Gauss-Seidel technique. Critical velocity of soil-foundation system has been determined. The parametric study conducted shows the influence of applied load, relative compressibility of soils, relative flexural rigidity, depth of placement of geocell, damping in the system and velocity of load on the response of rail and geocell reinforcement. Also, a sensitivity study has been carried out and it has been observed that sensitivity of the maximum positive response of the top beam towards variation in magnitude of applied load, relative compressibility of soil and relative flexural rigidity of beams is more as compared to other model parameters.

Keywords: Double beam model, rails, geocell, moving load.

1. INTRODUCTION

Increased speed of modern transportation systems leads to increased movement of rails and amplified vibrations. In some cases, improper land may be encountered during the alignment of such systems. This led to the introduction of ground improvement techniques in railways and highways. Some techniques like reinforcing soil with the help of geocell have been an area of interest in the field of transportation geotechnics since its development by U.S. Army Corps of Engineers to enhance vehicular mobility over loose sandy subgrade (Webster and Alford, 1978). The superiority of geocell layer in reducing differential deformations of the ground over other available geosynthetic reinforcements has been established in a few research works (Dash et al., 2004; Latha et al., 2010). By means of experimental and numerical studies, researchers have explored its influence on the response of railroads, paved or unpaved road system (Cowland and Wong, 1993; Fakher and Jones, 2001; Emersleben and Meyer, 2008; Thakur et al., 2012; Yang et al., 2012; Leshchinsky and Ling, 2013; Biabani et al., 2016; Zarembski et al., 2017; Satyal et al., 2018). Raymond (2002) and Indraratna et al. (2015) conducted experimental tests which indicated the significance of bending stiffness of the reinforcement layer. On account of this, some numerical studies modelled geocell reinforcement as a finite beam having finite bending stiffness (Fakher and Jones, 2001; Maheshwari and Viladkar, 2009; Zhang et al., 2009, 2010, 2018; Maheshwari and Babu, 2017). Therefore, rails constructed over geocell reinforced ground can be treated as a double beam model which has also been extensively used to apprehend the response of other engineering systems (Hussein and Hunt, 2006; Yuan et al., 2009; Auersch, 2012; Mohammadzadeh et al., 2014; Deng et al., 2017).

Many studies have been reported where response of rails has been studied by idealizing the problem as an infinite beam on one or two parameter foundation system subjected to moving load at constant speed (Kenney, 1954; Fryba, 1972; Kerr, 1974; Saito and Terasawa, 1980; Duffy, 1990; Jaiswal and Iyengar, 1997; Mallik et al., 2006; Dimitrovová, 2010; Ang and Dai, 2013; Basu and Rao, 2013). However, none of the above studies considered the case of improved ground, thus, limiting their applicability in problems for poor/soft soil foundation. In order to address this issue, Maheshwari and Khatri (2013) included geosynthetic reinforcement and stone columns modelled as a rough elastic membrane and stiffer spring respectively in the analysis. However, for a moving load problem on improved ground, the bending stiffness of the reinforcement has not been explored much. In view of this, an attempt has been made in the present study to analyze rails resting on geocell reinforced earth bed under a point load moving with constant velocity by means of a double beam model where the lower beam with finite bending stiffness represents geocell.

2. PROBLEM DEFINATION

Figure 1(a) describes the longitudinal rail section, where rails resting on granular layer placed on top of the soil system with geocell inclusion have been subjected to load Q moving with constant velocity v. The model includes a top and a bottom beam representing rails and geocell with infill material having flexural rigidity E_1I_1, E_2I_2 and mass per unit length ρ_1, ρ_2 respectively. The lower reinforcing beam (composite beam for geocell with infill soil) has been assumed having zero frictional surfaces as no substantial influence would be observed on the maximum deflection values due to this consideration (Maheshwari et al. 2005; Zhang et al. 2018). The granular layer thickness h exists between these two infinite beams idealised by Pasternak shear layer with shear modulus G, compressibility, k_1 and viscous damping coefficient, c_1 (Figure 1(b)). A series of spring and dashpot, connected in parallel, having stiffness, k_2 and viscous damping, c_2 represents the underlying foundation soil. A uniform load $\gamma_1 h$ denoting the self weight of the granular layer has been considered acting on the bottom beam where γ_1 denotes unit weight of granular layer. The behaviour of this double beam model under the impact of moving load for the various parameters under consideration is to be found out.

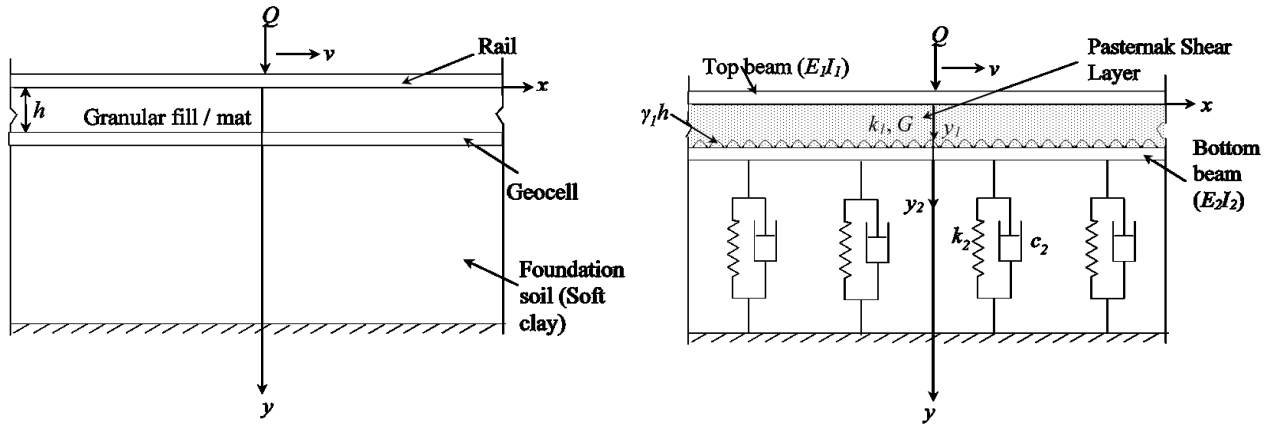

(a) Longitudinal section of rail lying on reinforced earth bed (b) Conceptualization of the problem

Figure 1. Statement of the problem.

3. ANALYSIS

3.1 Governing differential equations of motion

The governing equations of motion for the top and the bottom beam (Fig. 1(b)) can be developed by considering differential element of each beam and employing D'Alembert's principle. Equilibrium of forces in the vertical direction for these elements along with the relationship of bending moment and shear force when substituted gives the generalized equations of motion for both the beams which can be expressed as follows:

$$E_1I_1\frac{\partial^4 y_1}{\partial x^4}+\rho_1\frac{\partial^2 y_1}{\partial t^2}+c_1\frac{\partial(y_1-y_2)}{\partial t}+k_1(y_1-y_2)-Gh\frac{\partial^2(y_1-y_2)}{\partial x^2}=Q(x,t) \quad [1]$$

and

$$E_2I_2\frac{\partial^4 y_2}{\partial x^4}+\rho_2\frac{\partial^2 y_2}{\partial t^2}+c_2\frac{\partial y_2}{\partial t}+k_2y_2-\left[c_1\frac{\partial(y_1-y_2)}{\partial t}+k_1(y_1-y_2)-Gh\frac{\partial^2(y_1-y_2)}{\partial x^2}\right]=\gamma_1 h \quad [2]$$

where, y_1 and y_2 denote the deflection of the top and bottom beams respectively, x, represents the space coordinate at any time, t.

3.2 Solution of the developed equation system

In order to simplify the analysis, the system has been assumed to be in quasi-stationary state, i.e. after sufficiently long travel time moving load becomes independent of time. In order to incorporate this state, the system has been converted for a uniformly moving space co-ordinate by defining a variable ξ as, ξ=x-vt. Equations 1 and 2 can then be expressed in this transformed plane of reference as

$$E_1I_1\frac{d^4y_1}{d\xi^4}+\rho_1v^2\frac{d^2y_1}{d\xi^2}-c_1v\frac{d(y_1-y_2)}{d\xi}+k_1(y_1-y_2)-Gh\frac{d^2(y_1-y_2)}{d\xi^2}=Q(\xi) \quad [3]$$

and

$$E_2I_2\frac{d^4y_2}{d\xi^4}+\rho_2v^2\frac{d^2y_2}{d\xi^2}-c_2v\frac{dy_2}{d\xi}+k_2y_2-\left[-c_1v\frac{d(y_1-y_2)}{d\xi}+k_1(y_1-y_2)-Gh\frac{d^2(y_1-y_2)}{d\xi^2}\right]=\gamma_1h \quad [4]$$

Equations 3 and 4 can be written in terms of dimensionless parameters using the following non-dimensional terms:

$$\xi^*=\frac{\xi}{L};\ Y_1=\frac{y_1}{L};\ \rho_1^*=\frac{\rho_1v^2}{k_1L^2};\ \rho_2^*=\frac{\rho_2v^2}{k_2L^2};\ I_1^*=\frac{E_1I_1}{k_1L^4};\ I_2^*=\frac{E_2I_2}{k_2L^4};\ c_1^*=\frac{c_1v}{k_1L};\ c_2^*=\frac{c_2v}{k_2L};\ Q^*=\frac{Q}{k_1L^2};\ G^*=\frac{Gh}{k_1L^2};\ \gamma_1^*=\frac{\gamma_1}{k_2};\ H=\frac{h}{L};$$

$$r=\frac{k_1}{k_2};\ R=\frac{E_1I_1}{E_2I_2}$$

where L is the half-length of beams considered. Therefore, the governing differential equations 3 and 4 in the non-dimensional form can be written as

$$\frac{d^4Y_1}{d\xi^{*4}}+\frac{\rho_1^*}{I_1^*}\frac{d^2Y_1}{d\xi^{*2}}+\frac{(Y_1-Y_2)}{I_1^*}-\frac{c_1^*}{I_1^*}\frac{d(Y_1-Y_2)}{d\xi^*}-\frac{G^*}{I_1^*}\frac{d^2(Y_1-Y_2)}{d\xi^{*2}}=\frac{Q^*(\xi^*)}{I_1^*d\xi^*} \quad [5]$$

and

$$\frac{d^4Y_2}{d\xi^{*4}}+\frac{\rho_2^*}{I_2^*}\frac{d^2Y_2}{d\xi^{*2}}-\frac{c_2^*}{I_2^*}\frac{dY_2}{d\xi^*}+\frac{Y_2}{I_2^*}-\frac{r}{I_2^*}\left[(Y_1-Y_2)-c_1^*\frac{d(Y_1-Y_2)}{d\xi^*}-G^*\frac{d^2(Y_1-Y_2)}{d\xi^{*2}}\right]=\frac{\gamma_1^*H}{I_2^*} \quad [6]$$

The developed governing differential equations have been converted to finite difference form using central difference method which has been presented for any internal node, i as:

$$Y_{1,i}=\frac{1}{A_2}\left[\frac{Q_i^*(\Delta\xi^*)^3}{I_1^*}-Y_{1,i+2}-A_1Y_{1,i+1}-A_3Y_{1,i-1}-Y_{1,i-2}-A_4Y_{2,i+1}-A_5Y_{2,i}-A_6Y_{2,i-1}\right] \quad [7]$$

and

$$Y_{2,i}=\frac{1}{B_2}\left[\frac{\gamma_1^*H(\Delta\xi^*)^4}{I_2^*}-Y_{2,i+2}-B_1Y_{2,i+1}-B_3Y_{2,i-1}-Y_{2,i-2}-B_4Y_{1,i+1}-B_5Y_{1,i}-B_6Y_{1,i-1}\right] \quad [8]$$

where, $A_1=\frac{1}{I_1^*}\left[-4I_1^*+\rho_1^*(\Delta\xi^*)^2-0.5c_1^*(\Delta\xi^*)^3-G^*(\Delta\xi^*)^2\right];\ A_2=\frac{1}{I_1^*}\left[6I_1^*-2\rho_1^*(\Delta\xi^*)^2+(\Delta\xi^*)^4+2G^*(\Delta\xi^*)^2\right];$

$A_3=\frac{1}{I_1^*}\left[-4I_1^*+\rho_1^*(\Delta\xi^*)^2+0.5c_1^*(\Delta\xi^*)^3-G^*(\Delta\xi^*)^2\right];\ A_4=\frac{1}{I_1^*}\left[0.5c_1^*(\Delta\xi^*)^3+G^*(\Delta\xi^*)^2\right];\ A_5=\frac{1}{I_1^*}\left[-(\Delta\xi^*)^4-2G^*(\Delta\xi^*)^2\right];$

$A_6=\frac{1}{I_1^*}\left[-0.5c_1^*(\Delta\xi^*)^3+G^*(\Delta\xi^*)^2\right];\ B_1=\frac{1}{I_2^*}\left[-4I_2^*+\rho_2^*(\Delta\xi^*)^2-0.5c_2^*(\Delta\xi^*)^3+r\left\{-0.5c_1^*(\Delta\xi^*)^3-G^*(\Delta\xi^*)^2\right\}\right];$

$B_2=\frac{1}{I_2^*}\left[6I_2^*-2\rho_2^*(\Delta\xi^*)^2+(\Delta\xi^*)^4+r\left\{(\Delta\xi^*)^4+2G^*(\Delta\xi^*)^2\right\}\right];$

$B_3=\frac{1}{I_2^*}\left[-4I_2^*+\rho_2^*(\Delta\xi^*)^2+0.5c_2^*(\Delta\xi^*)^3+r\left\{0.5c_1^*(\Delta\xi^*)^3-G^*(\Delta\xi^*)^2\right\}\right];\ B_4=\frac{r}{I_2^*}\left[0.5c_1^*(\Delta\xi^*)^3+G^*(\Delta\xi^*)^2\right];$

$B_5=\frac{r}{I_2^*}\left[-(\Delta\xi^*)^4-2G^*(\Delta\xi^*)^2\right];\ B_6=\frac{r}{I_2^*}\left[-0.5c_1^*(\Delta\xi^*)^3+G^*(\Delta\xi^*)^2\right]$

3.3 Boundary Conditions

In order to represent the beams of infinite length sufficient length of the beam has been considered so that the variation in central load would have no effect on the deflection profile at the edges of the beam (Selvadurai, 1979). The boundary conditions for the purpose of determining the response of the idealized rail-soil dynamic system has been assumed according to Vlasov and Leontiev (1966). The non-dimensional form of these equations can be expressed as:

For the top beam

$$\left.\begin{aligned}\frac{d^3Y_1}{d\xi^{*3}} - \frac{G^*}{I_1^*}\frac{d(Y_1 - Y_2)}{d\xi^*} = 0\\ \frac{d^2Y_1}{d\xi^{*2}} = 0\end{aligned}\right\} \quad [9]$$

For the bottom beam

$$\left.\begin{aligned}\frac{d^3Y_2}{d\xi^{*3}} + \frac{rG^*}{I_2^*}\frac{d(Y_1 - Y_2)}{d\xi^*} = 0\\ \frac{d^2Y_2}{d\xi^{*2}} = 0\end{aligned}\right\} \quad [10]$$

3.4 Convergence Criterion and choice of parametric values

The algorithm of the above discussed mathematical model has been developed using MATLAB to determine the response. The entire stretch ($-L \le x \le L$) has been discretized in N number of nodes and equations 7 and 8 has been defined for each node. The boundary conditions expressed in equations 9 and 10 has been utilized to determine the unknown nodal deflection values at the edges of the beams. An initial value has been assumed for the deflections at all the internal nodes, followed by employing Gauss Seidel iterative method to find the required response.

For the analysis, 2001 nodes have been considered as the response of the beams have been negligibly affected (less than 0.5 %) on increasing the nodes from 2001 to 4001. The criterion adopted for the convergence test has been defined as follows:

$$\left.\begin{aligned}\left|\frac{Y_{1,i}^z - Y_{1,i}^{z-1}}{Y_{1,i}^z}\right| < \varepsilon\\ \left|\frac{Y_{2,i}^z - Y_{2,i}^{z-1}}{Y_{2,i}^z}\right| < \varepsilon\end{aligned}\right\} \quad [11]$$

for all i, where z denotes the current iteration and ε represents the tolerance factor which has been considered as 10^{-10} for the present analysis.

The input parameters used in the analysis has been considered as per the Indian railroad conditions and details of the same have been presented in Table 1. The viscous damping (c_1 and c_2) has been expressed in terms of damping ratios as shown in the following relationships using the concept of critical damping:

$$c_1 = 2\zeta_1\sqrt{k_1\rho_1} \text{ and } c_2 = 2\zeta_2\sqrt{k_2\rho_2} \quad [12]$$

3.5 Validation

In absence of any experimental data, the adopted solution technique has been verified by comparing the results of the present study with those of Hussein and Hunt (2006) where response of similar double beam model has been obtained by using Fourier Transformation technique. Considering the properties of sandwiched layer between the two beams to be in accordance with the rail pads, the present algorithm and methodology have been found to produce similar results

comparable to those obtained by Hussein and Hunt (2006) as shown in Fig. 2 for set of input parameters mentioned in the figure. Thus, validation of the adopted methodology and solution technique has been established.

Table 1. Input Parameters.

Parameters	Value	unit
Applied load (Q)	100-250	kN
Mass per unit length of top beam (ρ_1)	60	kg/m
Mass per unit length of bottom beam (ρ_2)	43 (Indraratna et al. 2015)	kg/m
Relative compressibility of soil ($r = k_1/k_2$)	1-20	-
Relative flexural rigidity of beams ($R = E_1I_1/E_2I_2$)	2400-4800	-
Damping ratio (ζ)	0-25 (Vucetic and Dorby 1991)	%
Velocity (v)	40-160	m/s

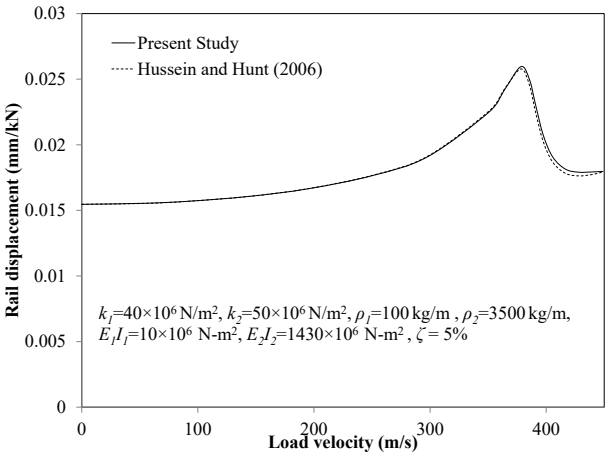

Figure 2. Validation of the proposed solution technique

4. RESULTS AND DISCUSSION

4.1 Critical velocity of the system

On increasing the velocity of the moving load for the system, the maximum deflection of top beam has been found to increase. In this process, sudden rise in this maximum top beam deflection has been found at a particular value of velocity. Beyond this value of velocity, the solution of developed algorithm starts diverging indicating the velocity be equal to the critical velocity of the system. The values of critical velocities thus obtained for various values of relative compressibility of soil has been presented in Table 2. It has been found that as relative compressibility of soil increases from 1 to 20, the critical velocity of the system reduces from 200 m/s to 161 m/s, i.e. around 20% reduction. For initial variation of r from 1 to 2, the degree of this reduction in the critical velocity has been observed as 10% which on further increments of r reduces drastically with showing only 1% reduction for variation in r from 10 to 20 and becomes constant at higher value of r.

Table 2. Critical velocity at different relative compressibility of soil.

Relative compressibility of soil, r	1	2	5	10	20	50
Critical velocity (m/s)	200	181	168	163	161	161

4.2 Effect of moving load (Q)

Figures 3(a) and 3(b) present the influence of magnitude of moving load on the deflection and bending moment of the top beam for the input values mentioned in the figures. It has been found that reduction in Q value from 250 kN to 100 kN results in 59% and 60% reduction in the maximum positive deflection and bending moment of the top beam respectively. On approaching the lowest value of Q i.e. 100 kN, the maximum negative deflections of the top beam have been observed to disappear and entire deflection profile has been found to exist in the positive space of vertical coordinate axis. Similar observations have been observed for the bottom beam deflection.

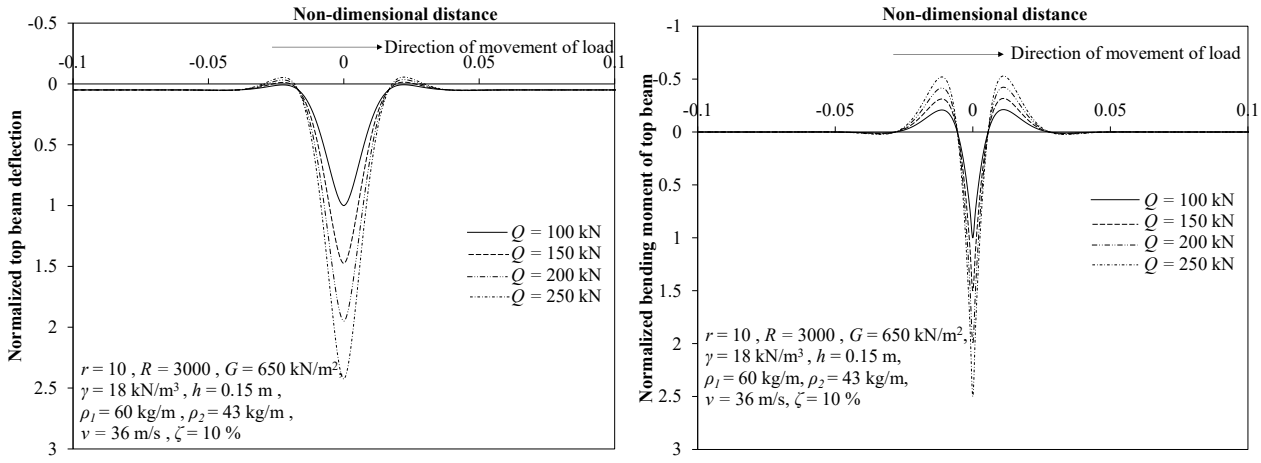

(a) Top beam deflection profile (b) Bending moment profile of the top beam

Figure 3. Influence of moving load.

4.3 Effect of relative compressibility of soil (r)

Figures 4(a) and 4(b) shows the effect of relative compressibility of soil on the deflection and bending moment of the top beam. On decreasing ratio r from 20 to 5, it has been found that the maximum positive deflection and bending moment of the top beam reduce by 61% and 27% respectively as lower values of r represent stiffer foundation soil.

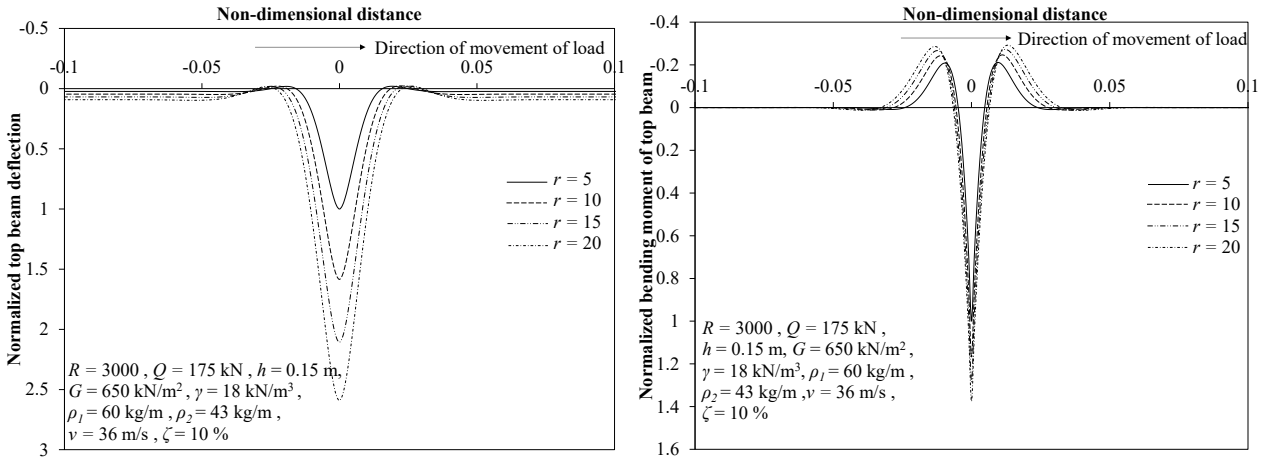

(a) Top beam deflection profile (b) Bending moment profile of the top beam

Figure 4. Influence of relative compressibility of soil.

4.4 Effect of relative flexural rigidity of the beams (R)

Figures 5(a) and 5(b) depict the effect of relative flexural rigidity on the deflection and bending moment profile of the top beam for the parameters mentioned in the figure. The maximum deflection of the top beam has been found to increase by 19% on decreasing the ratio R from 4800 to 2400. This may be due to the fact that a larger value of R denotes greater rigidity of top beam resulting in reduced deflections for the beam. However, maximum bending moment of the top beam decreases by 16% for similar variation in R, as the bending stiffness reduces on decreasing R.

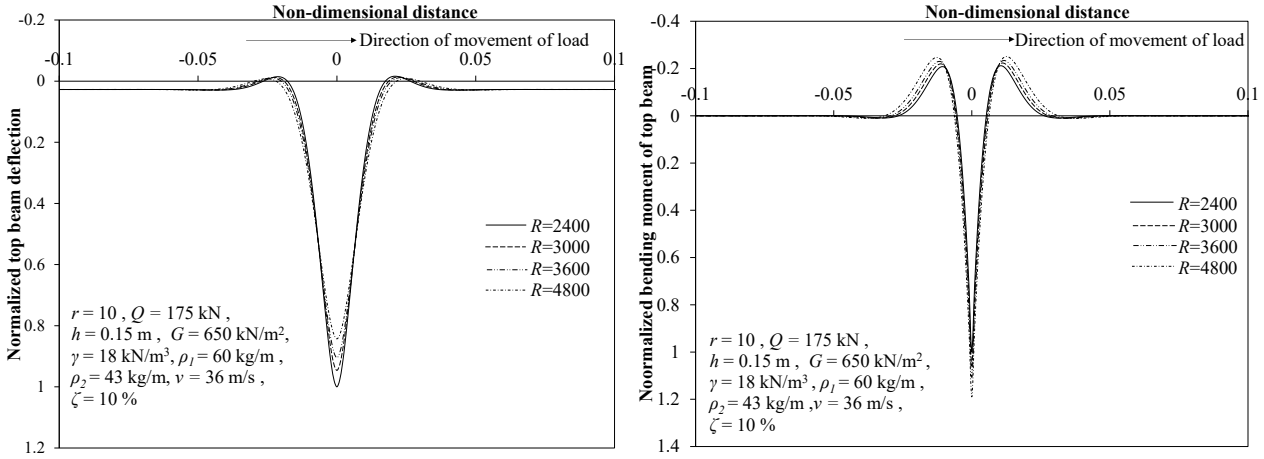

(a) Top beam deflection profile (b) Bending moment profile of the top beam

Figure 5. Influence of relative flexural rigidity of the beams.

4.5 Effect of location of bottom beam (h)

Figure 6 shows the effect of bottom beam placement depth on the deflection of the top beam for the input values mentioned in the figure. It has been found that the maximum deflection of the top beam increases by only 3% on increasing the depth of bottom beam from 0.5 m to 0.2 m. Also, the magnitude of minimum deflection has been observed to be very low and deflections of beams mostly lie in the positive space of vertical coordinate axis.

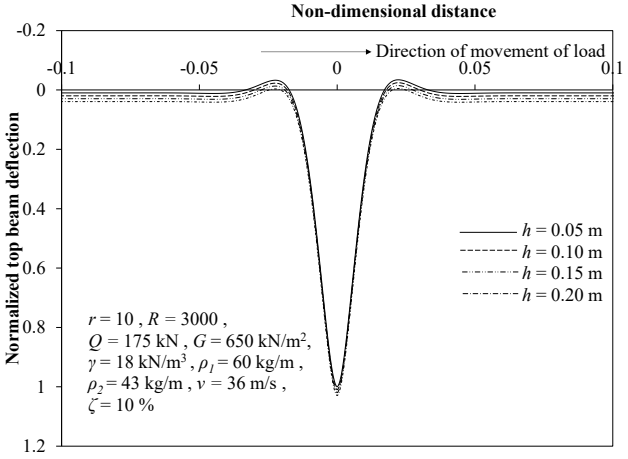

Figure 6. Influence of placement of bottom beam on top beam deflection.

4.6 Effect of velocity of applied load (v)

The outcome of variation in velocity of applied load on the top beam deflection has been presented in Figure. 7. The maximum positive deflection of both the top beam has been found to increase by 8% on increasing the velocity of load from 40 m/s to 160 m/s. It has to be noted that the degree of increase in deflection grows for every 40 m/s increment and the highest growth has been found for the final increment as the velocity approaches its critical value.

4.7 Effect of damping (ζ)

The effect of damping in the system on deflection profiles of the top beam has been investigated at higher value of velocity close to the critical velocity as at lower velocity no effect of variation was observed. On increasing damping ratio of the system from 0% to 25%, only 1% decrease in the positive deflection has been found. However, slight shift in the peak of the positive deflection behind the point of action of moving load has been observed. From the above investigation, it can be concluded that variation of damping in the system has negligible influence on the top beam deflection at both lower as well as higher value of velocities.

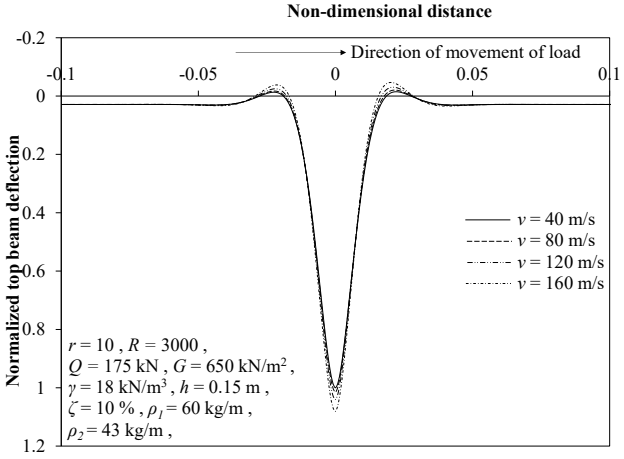

Figure 7. Influence of velocity of applied load on top beam deflection.

4.8 Sensitivity study

Sensitivity analysis has been conducted for following parametric values: Q = 175 kN , k_1= 150 MN/m^3 , E_1I_1 = 4470 kN-m^2 , R = 3000 , G = 650 kN/m^2 , γ = 18 kN/m^3 , ρ_1 = 60 kg/m , ρ_2 = 43 kg/m , ζ = 10 % , h = 0.15 m, v= 36 m/s. In order to the understand the sensitivity of maximum response of the system towards any parametric variation, maximum response of both the beams has been obtained for ± 20% and ± 10% variations from the mean value of considered parametric range. These results have been compared with the maximum response derived for mean value of the respective parameter and presented as percentage variations for maximum positive deflection and bending moment of both beams as shown in Figures 9(a) and 9(b). It can be clearly apprehended from the figures that sensitivity of the maximum positive response of the beams towards variation in magnitude of applied load, relative compressibility of soil and relative flexural rigidity of beams have been found to be significant compared to other parameters.

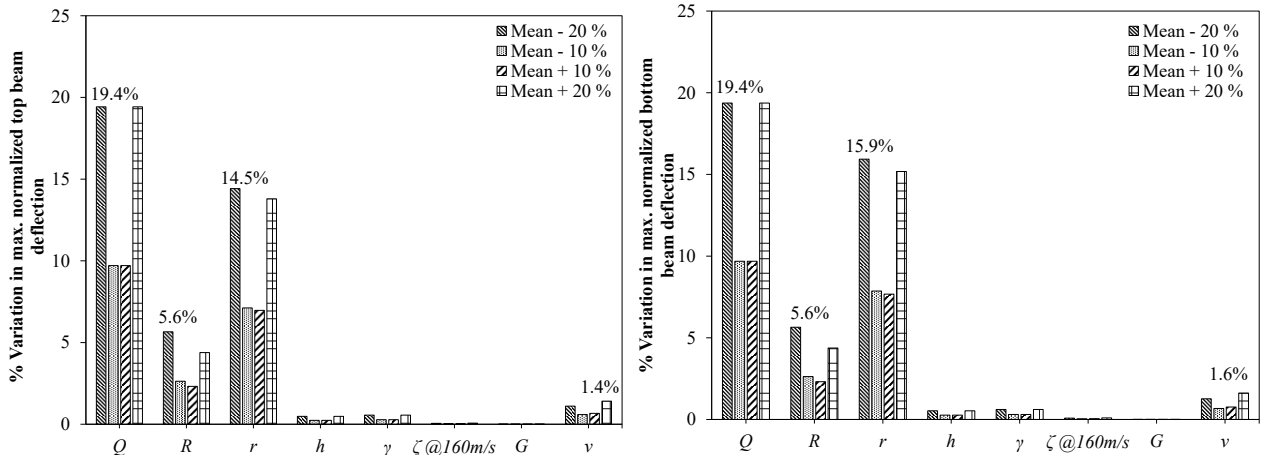

(a) Top beam deflection in positive direction (b) Bottom beam deflection in positive direction

Figure 9. Sensitivity analysis of maximum responses.

5. CONCLUSIONS

In the study, a simple mathematical model to determine the response of rails on geocell reinforced earth beds subjected to moving concentrated load has been studied. Detailed parametric and sensitivity analysis has been conducted to arrive at the following general conclusions:

- Critical velocity of the system has been presented for different values of relative compressibility of soil (r) and it has been observed that this crucial value reduces on increasing the value of r and the rate of this reduction nullifies at higher values of r.
- It has been observed that magnitude of moving load, relative compressibility of soil and relative flexural rigidity has a significant influence on the deflection and bending moment profile of the rails presented in details with the help of non-dimensional charts.
- A relatively smaller effect due to variation in depth of placement of bottom beam and velocity of moving load has been found. It is worth mentioning that the rate of increment in maximum positive top beam deflection increases on increasing the velocity and greater increment has been observed near critical velocity of the system. Also, it has been noted that damping ratio contributes only in minor shift in peak of the maximum deflection even at higher value of velocity.
- The influence of all the parameters on the maximum top and bottom beam deflection has been summarized with the help of results of sensitivity study which clearly reflects that the responses are more sensitive towards variation in magnitude of moving load, relative compressibility of soil and relative flexural rigidity compared to all other parameters considered in the analysis.

REFERENCES

Ang, K. K., and Dai, J. (2013). Response analysis of high-speed rail system accounting for abrupt change of foundation stiffness. *Journal of Sound and Vibration*, 332(12):2954–2970.

Auersch, L. (2012). Dynamic Behavior of Slab Tracks on Homogeneous and Layered Soils and the Reduction of Ground Vibration by Floating Slab Tracks. *Journal of Engineering Mechanics*, 138(8):923–933.

Basu, D., and Rao, N. S. V. K. (2013). Analytical solutions for Euler – Bernoulli beam on visco-elastic foundation subjected to moving load. *International Journal for Numerical and Analytical Methods in Geomechanics*, 37(8):945–960.

Biabani, M. M., Indraratna, B., and Ngo, N. T. (2016). Modelling of geocell-reinforced sub-ballast subjected to cyclic loading. *Geotextiles and Geomembranes*, 44(4):489–503.

Cowland, J. W., and Wong, S. C. K. (1993). Performance of a road embankment on soft clay supported on a Geocell mattress foundation. *Geotextiles and Geomembranes*, 12(8):687–705.

Dash, S. K., Rajagopal, K., and Krishnaswamy, N. R. (2004). Performance of different geosynthetic reinforcement materials in sand foundations. *Geosynthetics International*, 11(1):35–42.

Deng, H., Chen, K., Cheng, W., and Zhao, S. (2017). Vibration and buckling analysis of double-functionally graded Timoshenko beam system on Winkler-Pasternak elastic foundation. *Composite Structures*, 160:152–168.

Dimitrovová, Z. (2010). A general procedure for the dynamic analysis of finite and infinite beams on piece-wise homogeneous foundation under moving loads. *Journal of Sound and Vibration*, 329(13):2635–2653.

Duffy, D. G. (1990). The Response of an Infinite Railroad Track to a Moving , Vibrating Mass. *Journal of Applied Mechanics Division*, ASME, 57(1):66–73.

Emersleben, A., and Meyer, N. (2008). The use of geocells in road constructions over soft soil: vertical stress and falling weight deflectometer measurements. *4th European Geosynthetics Conference*, Edinburgh, UK.

Fakher, A., and Jones, C. J. F. P. (2001). When the bending stiffness of geosynthetic reinforcement is important. *Geosynthetics International*, 8(5):445–460.

Fryba, L. (1972). *Vibration of Solids and Structures under Moving Loads*. Noordhoff Publishing, Groningen, Netherlands.

Hussein, M. F. M., and Hunt, H. E. M. (2006). Modelling of floating-slab tracks with continuous slabs under oscillating moving loads. *Journal of Sound and Vibration*, 297(1–2):37–54.

Indraratna, B., Biabani, M. M., and Nimbalkar, S. (2015). Behavior of Geocell-Reinforced Subballast Subjected to Cyclic Loading in Plane-Strain Condition. *Journal of Geotechnical and Geoenvironmental Engineering*, 141(1):04014081-1–16.

Jaiswal, O. R., and Iyengar, R. N. (1997). Dynamic response of railway tracks to oscillatory moving masses. *Journal of Engineering Mechanics Division*, ASCE, 123(7):753–757.

Kenney, J. T. J. (1954). Steady-state vibrations of beam on elastic foundation for moving load. *Journal of Applied Mechanics Division,* ASME, 21(4):359–364.

Kerr, A. D. (1974). The Stress and Stability Analyses of Railroad Tracks. *Journal of Applied Mechanics Division*, ASME, 41(4):841–848.

Latha, G. M., Nair, A., and Hemalatha, M. (2010). Performance of geosynthetics in unpaved roads. *International Journal of Geotechnical Engineering*, 4(2):151–164.

Leshchinsky, B., and Ling, H. I. (2013). Numerical modeling of behavior of railway ballasted structure with geocell confinement. *Geotextiles and Geomembranes*, 36:33–43.

Maheshwari, P., and Babu, G. L. S. (2017). Nonlinear Deformation Analysis of Geocell Reinforcement in Pavements. *International Journal of Geomechanics*, 17(6):04016144.

Maheshwari, P., Basudhar, P. K., and Chandra, S. (2005). The effect of prestressing force and interfacial friction on the settlement characteristics of beams on reinforced granular beds. Indian Geotechnical Journal, 35(3):283–298.

Maheshwari, P., and Khatri, S. (2013). Response of infinite beams on geosynthetic-reinforced granular bed over soft soil with stone columns under moving loads. *International Journal of Geomechanics*, 13(6):713–728.

Maheshwari, P., and Viladkar, M. N. (2009). A mathematical model for beams on geosynthetic reinforced earth beds under strip loading. *Applied Mathematical Modelling*, 33(4):1803–1814.

Mallik, A. K., Chandra, S., and Singh, A. B. (2006). Steady-state response of an elastically supported infinite beam to a moving load. *Journal of Sound and Vibration*, 291:1148–1169.

Mohammadzadeh, S., Esmaeili, M., and Mehrali, M. (2014). Dynamic response of double beam rested on stochastic foundation under harmonic moving load. *International Journal for Numerical and Analytical Methods in Geomechanics*, 38(6):572–592.

Raymond, G. P. (2002). Reinforced ballast behaviour subjected to repeated load. *Geotextiles and Geomembranes*, 20(1):39–61.

Saito, H., and Terasawa, T. (1980). Steady-state vibrations of a beam on a Pasternak Foundation for moving loads. *Journal of Applied Mechanics Division*, ASME, 47(4):879–883.

Satyal, S. R., Leshchinsky, B., Han, J., and Neupane, M. (2018). Use of cellular confinement for improved railway performance on soft subgrades. *Geotextiles and Geomembranes*, 46(2):190–205.

Selvadurai, A. P. S. (1979). *Elastic analysis of soil-foundation interaction*. Elsevier Scientific Publishing Company, Amsterdam, Netherlands.

Thakur, J. K., Han, J., Pokharel, S. K., and Parsons, R. L. (2012). Performance of geocell-reinforced recycled asphalt pavement (RAP) bases over weak subgrade under cyclic plate loading. *Geotextiles and Geomembranes*, 35:14–24.

Vlasov, V. Z., and Leontiev, U. N. (1966). *Beams, plates and shells on elastic foundations*. Israel Program for Scientific Translations, Jerusalem.

Vucetic, M., and Dobry, R. (1991). Effect of Soil Plasticity on Cyclic Response. *Journal of Geotechnical Engineering*, ASCE, 117(1):89–107.

Webster, S. L., and Alford, S. J. (1978). *Investigation of construction concepts for pavement across soft ground*. Rep. S-77-1, Soils and Pavements Laboratory, U.S. Army Engineer Waterways Experiment Station, Vicksburg, MS.

Yang, X., Han, J., Pokharel, S. K., Manandhar, C., Parsons, R. L., Leshchinsky, D., and Halahmi, I. (2012). Accelerated pavement testing of unpaved roads with geocell-reinforced sand bases. *Geotextiles and Geomembranes*, 32:95–103.

Yuan, J., Zhu, Y., and Wu, M. (2009). Vibration characteristics and effectiveness of floating slab track system. *Journal of Computers*, 4(12):1249–1254.

Zarembski, A. M., Palese, J., Hartsough, C. M., Ling, H. I., and Thompson, H. (2017). Application of Geocell Track Substructure Support System to Correct Surface Degradation Problems Under High-Speed Passenger Railroad Operations. *Transportation Infrastructure Geotechnology*, 4(4):106–125.

Zhang, L., Ou, Q., and Zhao, M. (2018). Double-beam model to analyze the performance of a pavement structure on geocell-reinforced embankment. *Journal of Engineering Mechanics*, 144(8):06018002-1–7.

Zhang, L., Zhao, M., Zou, X., and Zhao, H. (2009). Deformation analysis of geocell reinforcement using Winkler model. *Computers and Geotechnics*, 36(6):977–983.

Zhang, L., Zhao, M., Zou, X., and Zhao, H. (2010). Analysis of geocell-reinforced mattress with consideration of horizontal-vertical coupling. *Computers and Geotechnics*, 37(6):748–756.